

A new method to create initially mass segregated star clusters in virial equilibrium

L. Šubr^{1,2,3*}, P. Kroupa¹ and H. Baumgardt¹

¹*Argelander Institute for Astronomy (AIfA), Auf dem Hügel 71, D-53121 Bonn, Germany*

²*Astronomical Institute, Charles University, V Holešovičkách 2, CZ-18000 Praha, Czech Republic*

³*Astronomical Institute, Academy of Sciences, Boční II, CZ-14131 Praha, Czech Republic*

Accepted Received

ABSTRACT

Mass segregation stands as one of the most robust features of the dynamical evolution of self-gravitating star clusters. In this paper we formulate parametrised models of mass segregated star clusters in virial equilibrium. To this purpose we introduce mean inter-particle potentials for statistically described unsegregated systems and suggest a single-parameter generalisation of its form which gives a mass-segregated state. We describe an algorithm for construction of appropriate star cluster models. Their stability over several crossing-times is verified by following the evolution by means of direct N -body integration.

Key words: stellar dynamics – methods: statistical – methods: N -body simulations

1 INTRODUCTION

Observations show quite often an increased concentration of massive stars towards the centres of young star clusters (e.g. ONC – Hillenbrand & Hartmann 1998; NGC 2157 – Fischer et al. 1998; NGC 3603 – Stolte et al. 2006). This tendency, known as mass segregation, can be of different origin: Initial mass segregation is sometimes considered (e.g. Murray & Lin 1996, Bonnell & Bate 2006) as a consequence of the formation of massive stars preferably in the densest regions (i.e. the cores) of the parent gas clouds. On the other hand, the process of mass segregation is also known to be one of the most robust features of the two-body relaxation driven evolution of self-gravitating star clusters (Chandrasekhar 1942, Spitzer 1969).

Several approaches were developed to setup a star cluster in the state of mass segregation. Gunn & Griffin (1978), Capuzzo Dolcetta et. al (2005) and others based their setup on multi-component King models (King 1965, Da Costa & Freeman 1976) with stars separated into several mass classes which interact with each other via smoothed potentials. This approach relies on solving of non-linear set of Poisson equations, which is possible for limited number of components. A multimass models of star cluster with exact energy equipartition in the core, which also leads to mass segregation, was introduced by Mocchi (2006). Another approach used e.g. by McMillan & Vesperini (2007) relies on segregation produced by N -body integration of initially un-

segregated systems towards the segregated state, i.e. it is equivalent to a simple redefinition of time $t = 0$.

In this paper we describe a new class of models of star clusters with continuous stellar mass distributions and a parametrised degree of mass segregation. The models are motivated by a study of the process of mass segregation during dynamical evolution of a self-gravitating cluster, which is briefly described in the following Section. We show that mass segregation strongly manifests itself in the energy space. In Section 3 we introduce convenient characteristics of a statistically described ensemble and derive their form for the unsegregated state. We further introduce in a heuristic manner an alternative, single-parameter form of these quantities that gives constraints on the distribution function of a mass segregated system. Afterwards, we describe an algorithm for construction of the corresponding star cluster. In Section 4 we demonstrate the stability of the models by means of N -body integrations. Finally, Section 5 contains our conclusions.

2 MOTIVATION

The standard scenario of the dynamical evolution of an isolated cluster is shown in Figure 1. The cluster in this example is initiated as an unsegregated Plummer model which is then integrated numerically with the NBODY6 code (Aarseth 2003). We consider 20000 stars with masses in the range $0.2M_{\odot} < m < 50M_{\odot}$ following a power-law mass function with Salpeter index $\alpha = -2.35$. The stars are treated as point-mass particles interacting solely by means of grav-

* E-mail: subr@sirrah.troja.mff.cuni.cz

ity and, therefore, there is no intrinsic length-scale within the model. Hence, we introduce a characteristic length- and time-scale:

$$r_0 \equiv \frac{1}{4}GM_c^2/|E_{\text{tot}}| \quad \text{and} \quad t_0 \equiv r_0^{3/2}/\sqrt{GM_c} \quad (1)$$

by means of the cluster total mass, M_c , and the integral of the equations of motion, the total energy, E_{tot} . The results can be scaled to any length scale, provided the identities (1) between r_0 , t_0 , M_c and E_{tot} are fulfilled. For a Plummer sphere, i.e. the initial state of the example model, the half-mass radius of the cluster is $r_h = 0.77r_0$ and t_0 corresponds to the crossing time. In the following we assume physically plausible stellar masses, although only ratios m_i/M_c do matter from the theoretical point of view. For definiteness, our ‘canonical’ model presented in Fig. 1 has $M_c = 13200M_\odot$, which for $r_h = 1\text{pc}$ gives $r_0 = 1.3\text{pc}$ and $t_0 = 0.2\text{Myr}$.

During the pre-core collapse phase of the cluster evolution, massive stars sink to the centre, forming a tightly bound core. This process is visible either in terms of the contraction of the inner Lagrange radii, or in terms of a decrease of the specific potential energy of massive stars,

$$\tilde{U}(m_{\text{lim}}) = \frac{\sum_i U^i}{\sum_i m_i}, \quad m_i > m_{\text{lim}}, \quad (2)$$

where

$$U^i \equiv - \sum_{j \neq i}^N \frac{G m_i m_j}{|\mathbf{r}_i - \mathbf{r}_j|} \quad (3)$$

is the potential energy of the i -th star. Compared to the latter quantity, the specific kinetic energy, $\tilde{K}(m_{\text{lim}}) \equiv \sum K^i / \sum m_i$, of the same subset of stars shows a less pronounced evolution. At time $t \sim 50t_0$ the cluster reaches the state of core collapse. From that point onward, strong few-body interactions between the core stars occur, leading to the formation of massive binaries carrying a considerable fraction of the cluster potential energy and, at the same time, to high velocity ejections of massive stars. This process stops further contraction of the Lagrange radii. However, the potential energy of the subset of massive stars continues to decrease. Both the potential and the kinetic energy show large variations due to the dynamical formation and destruction of binaries during the post-core collapse phase; the average kinetic energy of the massive stars starts to increase systematically due to the ejections. Note, however, that all stars are still kept in the computation.

Another view of the redistribution of (potential) energy among the stars is presented in Fig. 2, where we plot the internal potential energy,

$$U_{\text{sub}}^i \equiv - \sum_{j=2}^i \sum_{k=1}^{j-1} \frac{G m_j m_k}{|\mathbf{r}_j - \mathbf{r}_k|}, \quad (4)$$

as a function of mass of an ordered subset of stars,

$$M_{\text{sub}}^i \equiv \sum_{j=1}^i m_j, \quad m_1 \geq m_2 \geq \dots \geq m_N, \quad (5)$$

at four different times. In an initial, unsegregated, state, U_{sub}^i should be proportional to the second power of M_{sub}^i which is clearly the case for the bottom line in Fig. 2. As time proceeds, the slope of the curve gets shallower, i.e. massive stars hold an increasing fraction of the potential energy.

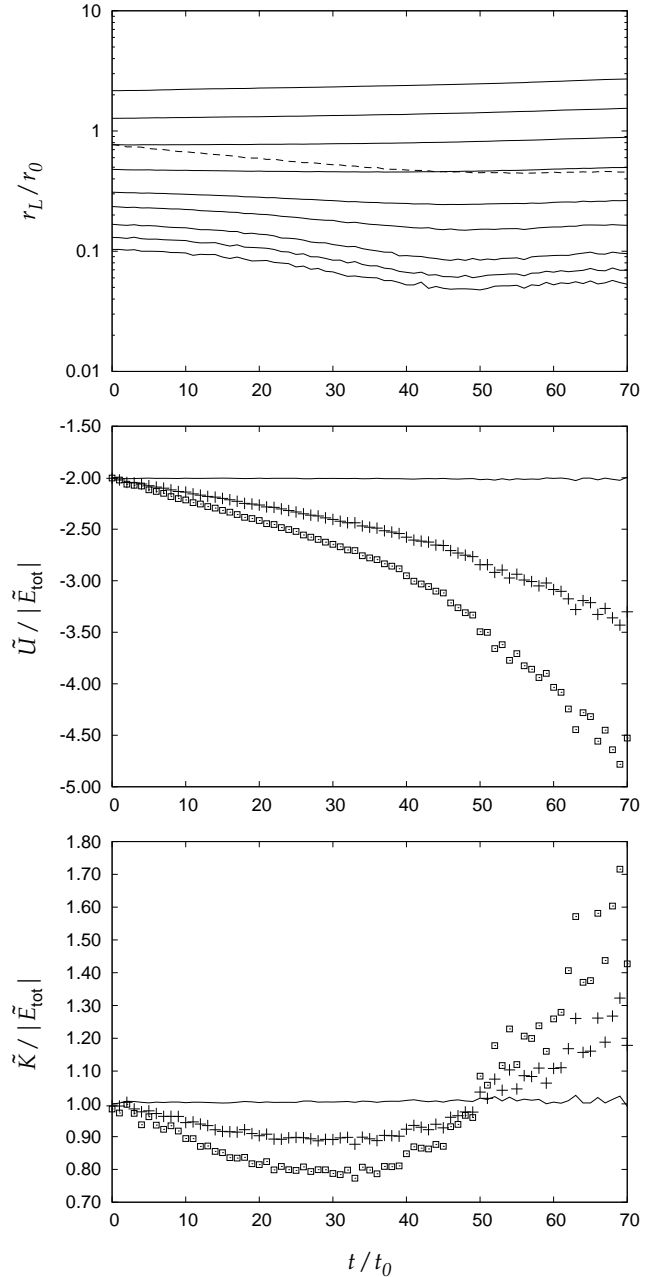


Figure 1. Evolution of characteristic quantities of an isolated cluster of 20000 stars. Top: Lagrange radii (0.5, 1, 2, 5, 10, 25, 50, 75 and 90 per cent of M_c) are plotted with solid lines; dashed line indicates half-mass radius of a subset of massive ($m > 5M_\odot$) stars. Middle and bottom: the specific potential, \tilde{U} , and specific kinetic, \tilde{K} , energy of a subset of stars in terms of specific total energy, $\tilde{E}_{\text{tot}} \equiv E_{\text{tot}}/M_c$. In all panels, solid lines represent quantities related to the whole cluster ($M_{\text{sub}} = M_c$), crosses correspond to the subset of stars with masses $m > 5M_\odot$ ($M_{\text{sub}} = 0.2M_c$) and open squares represent characteristics of subset with $m > 13M_\odot$ ($M_{\text{sub}} = 0.1M_c$). Plots are obtained as an average over 100 runs.

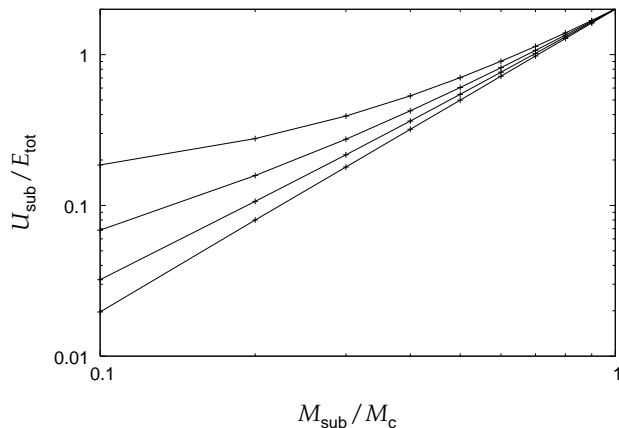


Figure 2. Internal potential energy of a subset of stars as a function of its mass. From bottom to top the lines correspond to $t = 0, 20, 40$ and $60t_0$. The plot represents an average over 100 different realisations of the cluster presented in Fig. 1.

At core collapse, the dependence can be approximated by another power-law function.

The apparent monotonical evolution of the potential energy of stars of different masses during the *whole* course of the cluster evolution motivates us to parametrise the mass segregation in energy rather than in configuration space.

3 MODEL

We consider an ensemble of N particles of masses m_i , $i = 1 \dots N$; we further denote with $M_c = \sum m_i$ the total mass of the cluster. The state of the system is determined by specifying N positions, \mathbf{r}_i , and conjugate momenta, \mathbf{p}_i , which altogether form a vector in a $6N$ -dimensional phase space. For large N such a ‘clean’ state of the system is usually either not known or is not of particular interest. The system is then in a statistical sense conveniently characterised by means of a distribution function, $D_N(\mathbf{r}_1, \mathbf{p}_1, \dots, \mathbf{r}_N, \mathbf{p}_N)$, i.e. a probability density to find it in a particular state. For definiteness, we assume D_N to be normalised to unity. The mean value of an arbitrary physical quantity related to the system is obtained by integration over the whole phase space,

$$\langle A \rangle = \int A(\mathbf{r}_1, \mathbf{p}_1, \dots, \mathbf{r}_N, \mathbf{p}_N) D_N(\mathbf{r}_1, \mathbf{p}_1, \dots, \mathbf{r}_N, \mathbf{p}_N) d\Omega, \quad (6)$$

with $d\Omega \equiv d^3\mathbf{r}_1 d^3\mathbf{p}_1 \dots d^3\mathbf{r}_N d^3\mathbf{p}_N$ representing the phase space volume element.

Specifying mean values of certain physical quantities is used to pose constraints on the form of the distribution function in the case when it is not known explicitly. We assume the mean total energy $\langle E_{\text{tot}} \rangle$ is given. Restricting ourselves to systems in virial equilibrium, it follows that mean values of the total kinetic and potential energies are in balance, $\langle K_{\text{tot}} \rangle = -\langle E_{\text{tot}} \rangle$, $\langle U_{\text{tot}} \rangle = 2\langle E_{\text{tot}} \rangle$. We further assume that the system is characterised by the mean potential energy between each two particles ($i \neq j$),

$$\langle U^{ij} \rangle \equiv - \int \frac{G m_i m_j}{|\mathbf{r}_i - \mathbf{r}_j|} D_N(\mathbf{r}_1, \mathbf{p}_1, \dots, \mathbf{r}_N, \mathbf{p}_N) d\Omega. \quad (7)$$

This quantity implies that the mean potential energy of the i -th particle is

$$\langle U^i \rangle = \sum_{j \neq i}^N \langle U^{ij} \rangle \quad (8)$$

and the mean ‘internal’ potential energy of a subset of particles is

$$\langle U_{\text{sub}}^i \rangle \equiv \sum_{j=2}^i \sum_{k=1}^{j-1} \langle U^{jk} \rangle. \quad (9)$$

The latter quantity will play an important role in the algorithm described below. In order to be unique, definition (9) requires specification of the order of the particles in the set. Hence, we recall that we assume $m_1 \geq m_2 \geq \dots \geq m_N$.

In order to take advantage of integral calculus, we will use replacements of summations:

$$\sum_{i=a}^b \rightarrow \int_a^b d\ell \iff \int_{M_{\text{sub}}^a}^{M_{\text{sub}}^b} \frac{dM'_{\text{sub}}}{m_i}. \quad (10)$$

Here, we use greek symbols to denote ‘‘continuous summation index’’. The equivalence in (10) can be understood as an analogy to the discrete increment $\Delta M_{\text{sub}}^i = m_i \Delta N$, where $\Delta N = 1$. This trick introduces some error, in particular for small values of a and b and steep mass functions. Nevertheless, it is useful to provide rather robust relations between individual quantities.

3.1 Unsegregated state

A commonly used scheme for construction of a cluster in a completely mixed (unsegregated) state is based on uncorrelated drawing of positions, \mathbf{r}_i , and velocities, $\mathbf{v}_i \equiv \mathbf{p}_i/m_i$, of individual stars according to a mass-independent single-particle distribution function $f(\mathbf{r}, \mathbf{v})$. This corresponds to the distribution function D_N in the form

$$D_N(\mathbf{r}_1, \mathbf{p}_1, \dots, \mathbf{r}_N, \mathbf{p}_N) d\Omega = \prod_{i=1}^N f(\mathbf{r}_i, \mathbf{v}_i) d^3\mathbf{r}_i d^3\mathbf{v}_i \quad (11)$$

with normalisation $\int f(\mathbf{r}_i, \mathbf{v}_i) d^3\mathbf{r}_i d^3\mathbf{v}_i = 1$. For example, in case of a Plummer model,

$$f(\mathbf{r}, \mathbf{v}) = \frac{24\sqrt{2}}{7\pi^3} \frac{r_p^2}{(GM_c)^5} (-\mathcal{E})^{7/2} \quad (12)$$

for $\mathcal{E} < 0$ and $f(\mathbf{r}, \mathbf{v}) = 0$ otherwise. Here, r_p represents the characteristic radius of the Plummer sphere and

$$\mathcal{E} \equiv \frac{1}{2}v^2 - \frac{GM_c}{r_p} \frac{1}{\sqrt{1 + (r/r_p)^2}} \quad (13)$$

is the specific energy of an individual particle.

Regardless of the particular form of $f(\mathbf{r}, \mathbf{v})$, from symmetries of the distribution function (11) it directly comes out that the mean potential energy between two particles has to be a bilinear function of (and only of) their masses,

$$\begin{aligned} \langle U^{ij} \rangle &= -G m_i m_j \int \frac{f(\mathbf{r}_i, \mathbf{v}_i) f(\mathbf{r}_j, \mathbf{v}_j)}{|\mathbf{r}_i - \mathbf{r}_j|} d^3\mathbf{r}_i d^3\mathbf{v}_i d^3\mathbf{r}_j d^3\mathbf{v}_j \\ &= -C G m_i m_j. \end{aligned} \quad (14)$$

The integral in (14) is an unknown constant C which is independent of indices i and j . Its value can be easily obtained

by evaluation of $\langle U_{\text{sub}}^i \rangle$, defined in (9), with the help of (10):

$$\begin{aligned} \langle U_{\text{sub}}^i \rangle &= \int_0^{M_{\text{sub}}^i} \frac{dM_{\text{sub}}^l}{m_l} \int_0^{M_{\text{sub}}^l} \frac{dM_{\text{sub}}^\kappa}{m_\kappa} \langle U^{l\kappa} \rangle \\ &= -CG \int_0^{M_{\text{sub}}^i} dM_{\text{sub}}^l \int_0^{M_{\text{sub}}^l} dM_{\text{sub}}^\kappa \\ &= -\frac{1}{2}CG \left(M_{\text{sub}}^i\right)^2. \end{aligned} \quad (15)$$

For $i = N$, i.e. $M_{\text{sub}}^i = M_c$, we require $\langle U_{\text{sub}}^i \rangle = \langle U_{\text{tot}} \rangle$, which implies:

$$C = \frac{2\langle U_{\text{tot}} \rangle}{GM_c^2}. \quad (16)$$

For completeness, the mean potential energy of the i -th particle, defined by formula (8) is

$$\langle U^i \rangle = \int_0^{M_c} \frac{dM_{\text{sub}}^l}{m_l} \langle U^{il} \rangle = 2\langle U_{\text{tot}} \rangle \frac{m_i}{M_c}. \quad (17)$$

3.2 Parametrisation of mass segregation

From N -body models (Fig. 1) we see that it is predominantly the *potential* energy which is transferred between the light and massive stars, while their average kinetic energy remains nearly unchanged during the course of the cluster evolution. Hence, we will attempt to determine mass segregation in terms of mean potentials. In particular, we assume the mean inter-particle potential in the form:

$$\langle U^{ij} \rangle = 2\langle U_{\text{tot}} \rangle \frac{m_i m_j}{M_c^2} \tilde{U}^{ij} \quad (18)$$

and consider several limitations to the term \tilde{U}^{ij} :

- (i) it has to be symmetric with respect to the indices i and j . Only then will the total potential energy of the cluster be independent of the order of summation;
- (ii) it has to be positive and decreasing with increasing values of indices i and j , so that massive stars (with lower indices) have lower specific potential energy;
- (iii) it should not depend explicitly on masses m_i and m_j . Otherwise, core collapse could not be obtained for a cluster of equal mass stars.

One of the simplest forms that fulfils these requirements is:

$$\langle U^{ij} \rangle = 2(1-S)^2 \langle U_{\text{tot}} \rangle \frac{m_i m_j}{M_c^2} \left(\frac{M_{\text{sub}}^i M_{\text{sub}}^j}{M_c^2} \right)^{-S} \quad (19)$$

with $S \geq 0$ being the *index of mass segregation*. In analogy to (15), formula (19) implies

$$\langle U_{\text{sub}}^i \rangle = \langle U_{\text{tot}} \rangle \left(\frac{M_{\text{sub}}^i}{M_c} \right)^{2-2S} \quad (20)$$

and

$$\langle U^i \rangle = 2(1-S) \langle U_{\text{tot}} \rangle \frac{m_i}{M_c} \left(\frac{M_{\text{sub}}^i}{M_c} \right)^{-S}. \quad (21)$$

Clearly, $S = 0$ corresponds to an unsegregated cluster while $S > 1$ would lead to a sign inconsistency of the potential energy of individual particles and $\langle U_{\text{tot}} \rangle$. Hence, only $S \in (0, 1)$ should be considered as a reasonable value. The power-law form of $\langle U_{\text{sub}}^i \rangle (M_{\text{sub}}^i)$ is in accord with our motivation by the pre-core collapse evolutionary stages as depicted in Fig. 2.

3.3 Building up the cluster

Formula (19) gives constraints on the distribution function of the cluster, although it does not determine it explicitly. The constraints expressed in terms of $\langle U_{\text{sub}}^i \rangle$ can, however, be used to construct¹ a corresponding star cluster by adding one by one the individual stars from the ordered set.

The position of each added star is generated randomly (with isotropically distributed orientation) according to some ‘underlying’ distribution function $n(r)$. The potential energy of the (sub)cluster, U_{sub}^i , is calculated and compared with the desired mean value determined by eq. (19) and (9). (In the numerical code we drop the integral approximation to calculate $\langle U_{\text{sub}}^i \rangle$ and evaluate it by means of summation in order to achieve better consistency.) If the difference $|U_{\text{sub}}^i - \langle U_{\text{sub}}^i \rangle|$ is smaller than some given limit², then we proceed to the next star in the set. Otherwise, we generate another position of the i -th star, until the match is adequate.

The method for construction of the cluster described here has to be considered as a way how to find *some* state conforming to the given N constraints. Hence, it is natural that the solutions do depend on the form of the underlying function used for generation of trial positions of added stars. The fewer trials are needed to find a matching position, the more likely is the final state close to a maximum of the distribution function D_N . By estimating contributions to the potential energy by individual particles (see Appendix A), we have found that a good underlying function (that needs on average less than 1.5 trials per particle) is given by:

$$n(r) \propto r^2 \left(r_p^2 (M_{\text{sub}}^i) + r^2 \right)^{-5/2} \quad (22)$$

with

$$r_p(M_{\text{sub}}^i) = \frac{3\pi}{32} \frac{GM_c^2}{|\langle U_{\text{tot}} \rangle|} \frac{1}{1-S} \left(\frac{M_{\text{sub}}^i}{M_c} \right)^{2S}. \quad (23)$$

For $S = 0$, $n(r)$ corresponds to the density of a Plummer model. Notice, however, that only for $S = 0$, the underlying distribution function is equivalent to the radial density profile of the cluster. The relation between the underlying distribution and the density profile of the obtained cluster is nontrivial due to the selection mechanism based on the check of U_{sub}^i vs. $\langle U_{\text{sub}}^i \rangle$ in each step.

Velocity distribution

At the end of the above procedure, positions and potentials of all particles are determined. In the next step we assign velocities to the stars such that the system is in a quasi-equilibrium state. As we assume the mean specific kinetic energy to be independent of the mass of the star, the distribution function of velocities has to be such that $\frac{1}{2} \langle v_i^2 \rangle = -\langle E_{\text{tot}} \rangle / M_c$. Furthermore, the velocity has to be correlated to the local gravitational potential, $V(r)$, e.g. it

¹ A numerical C-code `plumix` for generating the cluster according to the algorithm described here can be downloaded from the AlfA web page: <http://www.astro.uni-bonn.de>

² In particular, for definiteness of the examples presented below, we considered $|U_{\text{sub}}^i - \langle U_{\text{sub}}^i \rangle| < |\langle U_{\text{sub}}^i \rangle| / \sqrt{i+1}$ as a condition to accept the position of a particle.

has to fulfil $v \leq \sqrt{2|V(r)|}$ in order to get a gravitationally bound system.

We are motivated by the standard construction of the velocity distribution of a Plummer cluster (e.g. Aarseth, Hénon & Wielen 1974),

$$v(r) = q\sqrt{2|V(r)|}, \quad (24)$$

where $q \in (0, 1)$ is a random number drawn from the distribution function

$$n'(q) = q^2(1 - q^2)^{7/2}, \quad (25)$$

with mean square value, $\langle q^2 \rangle = \frac{1}{4}$. In the case of our models, the explicit form of $V(r)$ is not known, nevertheless, it can be replaced with U^i/m_i which is calculated for each particle in the first step of the procedure. As for $S \neq 0$,

$$\langle v_i^2 \rangle \propto \langle qU^i \rangle / m_i = \frac{1}{4} \langle U^i \rangle / m_i \quad (26)$$

is not independent of the particle index (mass), we cannot use directly the distribution (25). Instead, we consider a generalised form

$$n'(q; \beta) = q^2(1 - q^2)^\beta. \quad (27)$$

Then, $\langle q^2 \rangle(\beta)$ is a monotonically decreasing function, being singular at $\beta = -1$. Hence, if we find β (see Appendix B) such that

$$\langle q^2 \rangle = \frac{|E_{\text{tot}}| m_i}{|\langle U^i \rangle| M_c}, \quad (28)$$

formula (24) with q drawn from the distribution function (27) will give the velocity of the i -th particle with mean square value

$$\langle v_i^2 \rangle = \langle q^2 \rangle \langle 2|V^i| \rangle = \langle q^2 \rangle \frac{2|\langle U^i \rangle|}{m_i} = \frac{2|E_{\text{tot}}|}{M_c}, \quad (29)$$

as required. For $S = 0$ the method is equivalent to the standard scheme used for the Plummer model.

4 TESTS

Fig. 3 shows radial density profiles of three models with different values of the index S . In all cases, the clusters were built up with 20000 particles with masses according to the Salpeter power-law mass function used in Fig. 1. The case $S = 0$ corresponds to an unsegregated system. As the algorithm is very similar to a standard scheme for the Plummer model in this limit, the radial density profile obtains a characteristic shape with constant density core and outer parts with density falling as $r^{-5/2}$. Increasing the index of mass segregation leads to considerable changes of the structure of the cluster. In the inner part (approximately up to the half-mass radius) the density can be approximated by a power-law, $\rho(r) \propto r^{-1.25}$ and $\propto r^{-2}$ for $S = 0.25$ and $S = 0.5$, respectively. Note that in the latter case the density profile approximates the analytic solution of Lynden-Bell & Eggleton (1980) for core-collapsed (single-mass) star clusters (see also Baumgardt et al. 2003 for a numerical study of the parameters of core collapse).

Another view of the clusters' state, in terms of kinetic energy, is presented in Fig. 4. Here we plot the mean kinetic energy of stars within the inner region, $r < 0.05r_0$, as a function of their mass. In the unsegregated state, $S = 0$, the

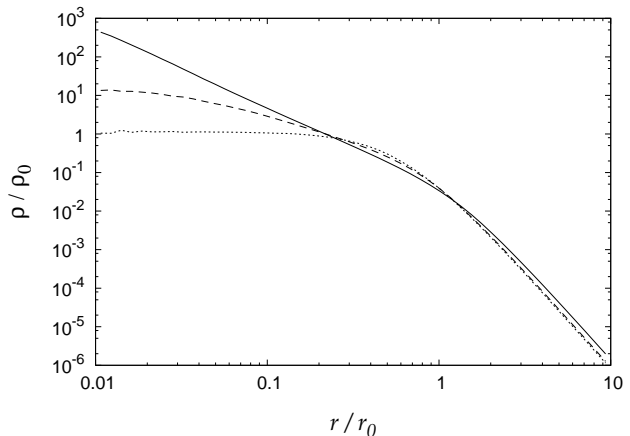


Figure 3. Radial mean density profile of three different models with $S = 0$ (dotted), $S = 0.25$ (dashed) and $S = 0.5$ (solid line). Clusters were built of 20000 particles with a Salpeter power-law mass function. In order to obtain smoothed density profiles even at very small radii, the profiles were obtained as an average of 20000 realisations with different initialisations of the random number generator. Half-mass radii of the clusters with different S are very similar ($r_h \approx 0.8r_0$; see Fig. 5 below). Density is expressed in units of $\rho_0 \equiv M_c/r_0^3$.

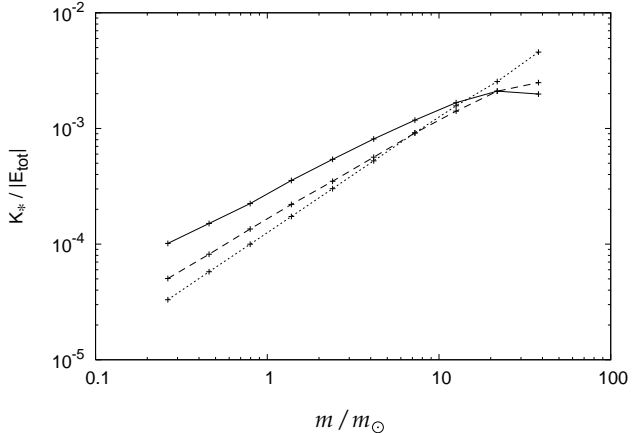


Figure 4. Mean kinetic energy in the core, $r_c < 0.05r_0$, as a function of the stellar mass. Models are identical to those in Fig. 3, i.e. dotted, dashed and solid lines correspond to $S = 0, 0.25$ and 0.5 , respectively. The kinetic energy was calculated for ten mass bins indicated with crosses.

velocity distribution function is independent of the mass of stars and, therefore, $K \propto m$ everywhere within the cluster, including its core. For the sake of simplicity of the model we have posed a constraint of $\langle K \rangle \propto m$ also for the mass segregated states. Nevertheless, according to eq. (24), the local mean kinetic energy depends on the particle mass. When placed at the same position, i.e. the same $V(r)$, a light star will have on average a higher specific kinetic energy than a massive one as its velocity will be drawn from the distribution (27) with a lower β , i.e. higher $\langle q^2 \rangle_\beta$ (note that index β of the velocity distribution depends on the index of the star, but it is independent of its position). Furthermore, the selection criterion in the first step of the algorithm

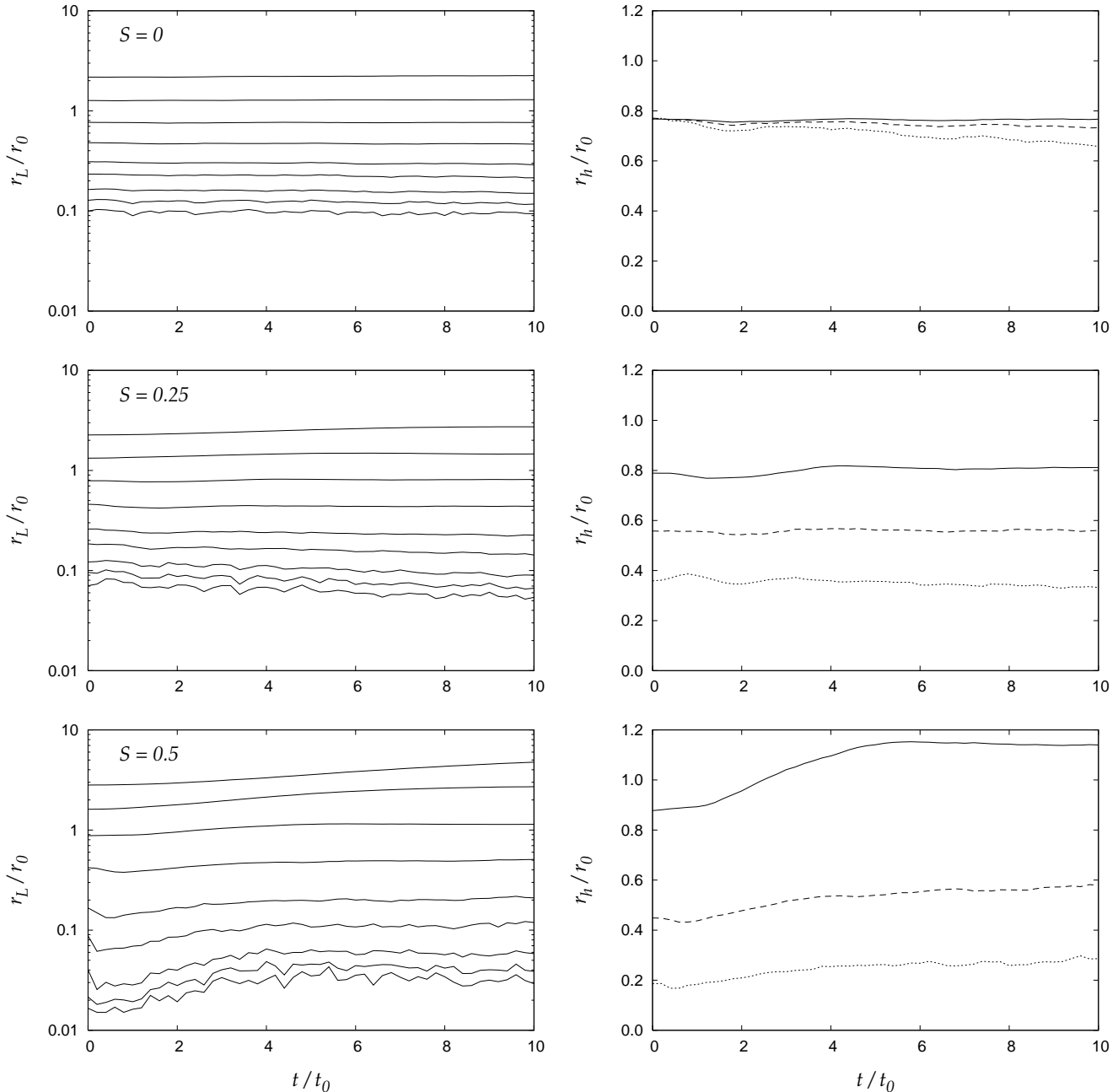


Figure 5. Left panels: evolution of the Lagrange radii (like in Fig. 1 individual lines correspond to 0.5, 1, 2, 5, 10, 25, 70, 75 and 90 per cent of the cluster mass) of clusters generated with different values of the index of mass segregation. The right panels show the evolution of the half-mass radii of the whole cluster (solid), for a subset of stars with $m > M_{\odot}$ (dashed) and a subset with $m > 5M_{\odot}$ (dotted line). In order to distinguish trends from random fluctuations, the plots represent averages of 20 runs with identical values of the model parameters.

allows low-mass stars to be placed in the innermost region extremely rarely³, that is only if they hit the local minima of $|V(r)|$. On the other hand, massive stars are allowed to enter local maxima of $|V(r)|$ which stands as a multiplicative factor in eq. (24). This effect slightly weakens the tendency

³ For $S = 0.5$ stars from the lowest mass bin, $m \in (0.2M_{\odot}, 0.35M_{\odot})$, represent less than 0.03% of the total number of stars within $0.05r_0$.

towards energy equipartition in the core which, however, still remains a generic feature of the mass segregated models as it is demonstrated in Fig. 4.

Dynamical evolution

To test the stability of the models, we have used them as initial conditions for N -body integrations. Results are presented in Fig. 5: The initially unsegregated system ($S = 0$) evolves rather smoothly without any apparent signs of in-

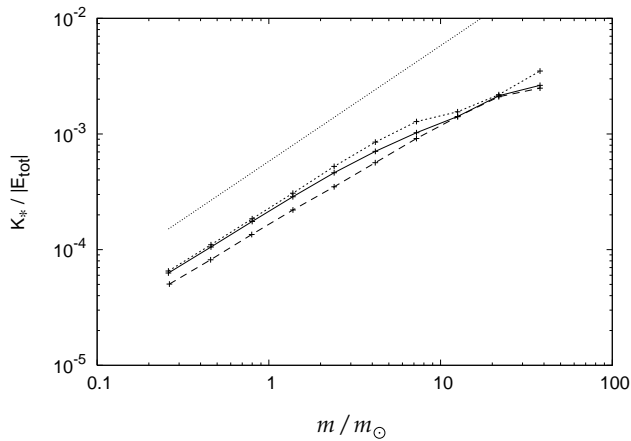


Figure 6. Mean kinetic energy in the core for the model with $S = 0.25$. Dashed line represents the initial (already mass segregated) state, i.e. it is identical to the dashed line in Fig. 4. Solid line is a snapshot at $t = 5t_0$ of that model integrated numerically. Dotted line corresponds to the model shown in Fig. 1 at $t = 50t_0$, evolving from an unsegregated state. Thin dotted line represents escape kinetic energy from the cluster centre.

stability. Due to the high mass ratio, the process of mass segregation can be observed already on the time scale of a few crossing times.

$S = 0.25$ gives a strongly segregated cluster. In this model the half-mass radius of stars heavier than $5mM_\odot$ contracts slightly, but it is already close to a saturated value. Note that its value is approximately one half of the half-mass radius of the whole cluster. This is in a good agreement with the model presented in Fig. 1 in the state of core collapse. In the right plot, which has a linear scale, we can see small initial oscillations of the half-mass radii which, however, are quickly damped. In general, this model can be considered as a quasi-stationary state very close to core collapse.

The model with $S = 0.5$ shows more significant initial oscillations as well as considerable overall expansion. It appears that for this value of S , the algorithm produces a virially hot system with $\langle K_{\text{tot}} \rangle \approx 0.55 \langle U_{\text{tot}} \rangle$. This means that the criterion for accepting a newly added star on a particular position, which is formulated in terms of $\langle U_{\text{sub}}^i \rangle$, does not reproduce the mean potential energy $\langle U^i \rangle$ with sufficient accuracy.

In order to test the stability of the models also in terms of the kinetic energy in the core, we show in Fig. 6 snapshots of the model with $S = 0.25$ at time $t = 0$ and $t = 5t_0$. We see that after a few crossing times the kinetic energy of the low mass stars settles at somewhat (approximately by a factor 1.3) higher values, while it remains nearly unchanged at the high-mass end. No further shift of the kinetic energy was observed for $t \gtrsim 5t_0$. Interestingly, the new state, which settles after a few crossing times, fits very well to the state of a model which was followed from an initially unsegregated state to the state of core collapse (model from Fig. 1 at $t = 50t_0$).

The escape kinetic energy from the core is linearly proportional to the stellar mass. Hence, in order to be bound to the cluster, light stars cannot have a kinetic energy equal to that of massive stars, i.e. the state of exact kinetic energy

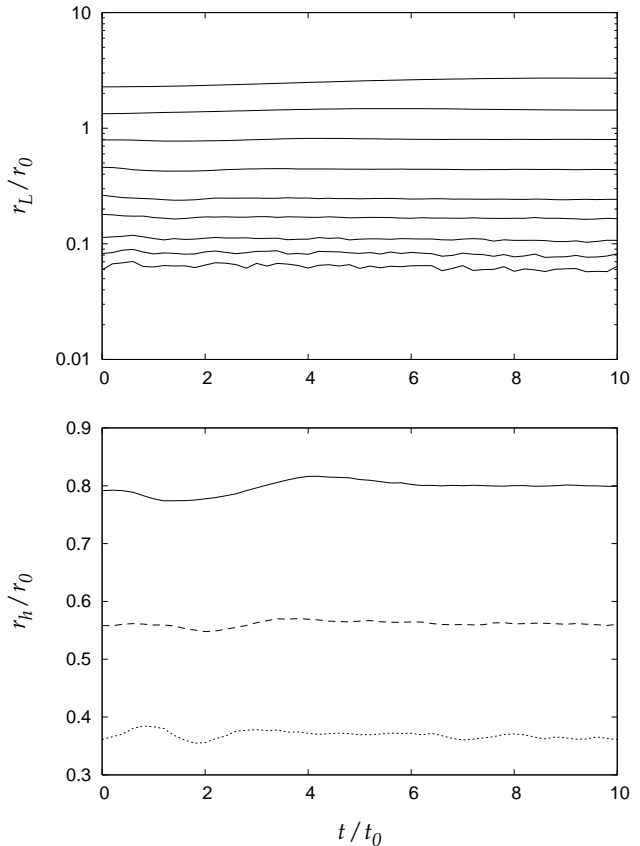


Figure 7. Top: evolution of the Lagrange radii for an initially mass segregated ($S = 0.25$) cluster of 100000 stars with a Salpeter mass function. Bottom: half-mass radius of the whole cluster and subsets with $m > M_\odot$ and $m > 5M_\odot$ are plotted with solid, dashed and dotted lines, respectively.

equipartition in the core is not possible even in the model with a rather high value of the index of mass segregation presented in Fig. 6.

Mass function dependence

The algorithm described in Sec. 3.3 does not depend explicitly on the mass function (i.e. it can be used for any set m_i). Nevertheless, its output is mass function dependent, as the constraints $\langle U_{\text{sub}}^i \rangle$ depend on particular values of m_i . We have performed tests with different sets in order to check the robustness of the algorithm.

First, we considered the same mass function as before (i.e. $m \in \langle 0.2, 50 \rangle$ and $\alpha = -2.35$) but now with 100000 particles. As we can see from Fig. 7, in terms of the characteristic radii the model with $S = 0.25$ evolves like its counterpart with 20000 particles, including the initial oscillations. A similar match was found also for different values of S , which we do not present here for the sake of brevity.

A model with 20000 stars and a more artificial mass function ($m \in \langle 0.1M_\odot, 10M_\odot \rangle$ and $\alpha = -1.35$) and mass segregation index $S = 0.25$ is presented in Fig. 8. Its behaviour in terms of Lagrange or half-mass radii is similar to the case with the Salpeter mass function. The radial density and kinetic energy profiles are also similar to those presented

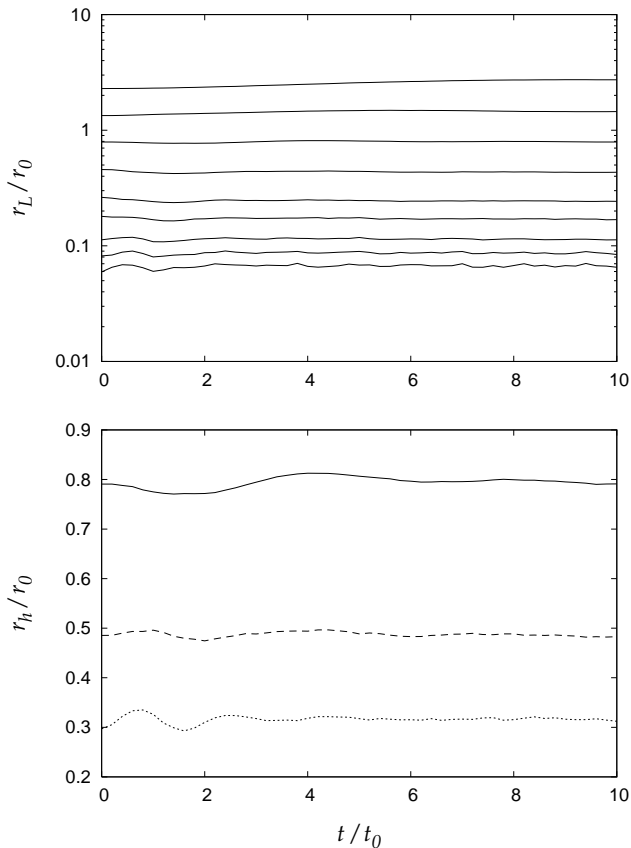


Figure 8. Evolution of Lagrange radii (the same fractions as in the previous figures are considered) of a model with shallow mass function ($\alpha = -1.35$, $m \in \langle 0.1M_{\odot}, 10M_{\odot} \rangle$). Half mass radii in the bottom panel correspond to the whole cluster (solid), $m > 5M_{\odot}$ ($M_{\text{sub}} = 0.38M_c$; dashed) and $m > 8M_{\odot}$ ($M_{\text{sub}} = 0.14M_c$; dotted line)

above. Hence, we can conclude that models with $S < 0.5$ are stable and their relaxational evolution is not influenced by apparently artificial effects.

In both cases presented in this section, the few most massive stars played a less important role in the cluster dynamics, compared to the ‘canonical’ models presented in Figs. 3 – 6. These models helped us to reveal the origin of a slight flattening of the density profile, which can be observed in the case of a Salpeter mass function for $S = 0.25$ (Fig. 3, dashed line). This effect is a demonstration of the dependence of $\langle U_{\text{sub}}^i \rangle$ on the masses of individual stars. In particular, $\langle U_{\text{sub}}^{i=2} \rangle$ determines the mean separation of the two heaviest particles, which is $\approx 0.03r_0$ for a Salpeter mass function, but $< 0.01r_0$ for the flatter one. Consequently, the mean density in this region stays approximately constant as the mass included is determined mainly by the two most massive stars.

5 CONCLUSIONS

We have introduced a way of parametrisation of self-gravitating systems in terms of mean inter-particle potentials. We have demonstrated that this approach can be used

for construction of quasi-stationary models of mass segregated star clusters. For the sake of simplicity, we have performed tests with simple power-law mass function. Nevertheless, the approach does not depend on a particular form of the mass function and the standard IMF (Kroupa 2001, 2007) can be used as an input. Notice also that even for a cluster of equal mass stars the algorithm will lead to a system with a desired level of ‘energy segregation’ which is in general the process that drives the star clusters towards core collapse.

Finally, let us remark that the index of mass segregation is likely to be related to the entropy. For $S = 0$ the system is highly symmetric in terms of $\langle U^{ij} \rangle$. On the other hand, in the limit of $S = 1$ it is required that all binding energy is carried by the two most massive particles, which is usually considered a state of maximal entropy of the self-gravitating system. We suggest that the statistical approach based on characterisation of the system by mean values of suitable physical quantities related to subsets of stars deserves further investigation, providing us, hopefully, with a deeper understanding of the thermodynamics of star clusters.

ACKNOWLEDGMENTS

We would like to thank Paolo Miocchi, for helpful comments to the paper. L.Š. gratefully appreciates a fellowship from the Alexander von Humboldt Foundation and the hospitality of the host institute (AIfA). This work was also supported by the DFG Priority Program 1177, the Centre for Theoretical Astrophysics in Prague and the Czech Science Foundation (ref. 205/07/0052).

APPENDIX A: UNDERLYING RADIAL DISTRIBUTION

The mean potential energy of a Plummer cluster of mass M_c and a characteristic radius r_p is

$$\langle U_{\text{tot}} \rangle = -\frac{3\pi}{32} \frac{GM_c^2}{r_p}. \quad (\text{A1})$$

The contribution of mass from the interval $\langle M_{\text{sub}}, M_{\text{sub}} + dM_{\text{sub}} \rangle$ is, approximately,

$$d\langle U_{\text{sub}} \rangle \approx -\frac{3\pi}{16} \frac{GM_{\text{sub}} dM_{\text{sub}}}{r_p} \quad (\text{A2})$$

(this relation is exact only for $r_p = \text{const}$). On the other hand, formula (20) implies

$$d\langle U_{\text{sub}} \rangle = (2 - 2S) \langle U_{\text{tot}} \rangle \left(\frac{M_{\text{sub}}^i}{M_c} \right)^{1-2S} \frac{dM_{\text{sub}}}{M_c}. \quad (\text{A3})$$

Combining (A2) and (A3) gives an estimate (23) for $r_p(M_{\text{sub}})$.

APPENDIX B: PARAMETRISATION OF THE VELOCITY DISTRIBUTION

The mean square value of a random number from an interval $\langle 0, 1 \rangle$ and probability density $n'(q; \beta) = q^2 (1 - q^2)^\beta$ is

$$\langle q^2 \rangle_\beta = I_\beta / J_\beta, \quad (\text{B1})$$

where

$$I_\beta \equiv \int_0^1 q^4 (1 - q^2)^\beta dq \quad (\text{B2})$$

and

$$J_\beta \equiv \int_0^1 q^2 (1 - q^2)^\beta dq. \quad (\text{B3})$$

Integrals (B2) and (B3) can be evaluated analytically for integer and half-integer $\beta \geq -\frac{1}{2}$ by means of recursive formulae:

$$I_\beta = \frac{2\beta}{5 + 2\beta} I_{\beta-1} \quad \text{with} \quad I_{-1/2} = \frac{3\pi}{16}, \quad I_0 = \frac{1}{5} \quad (\text{B4})$$

and

$$J_\beta = \frac{2\beta}{5 + 2\beta} J_{\beta-1} \quad \text{with} \quad J_{-1/2} = \frac{\pi}{4}, \quad J_0 = \frac{1}{3}. \quad (\text{B5})$$

In order to find β giving $\langle q^2 \rangle$ according to equation (28) we start from $\beta = -1/2$ and evaluate recursively $\langle q^2 \rangle_\beta$ until upper and lower limits $\langle q^2 \rangle_{\beta_1} \leq \langle q^2 \rangle \leq \langle q^2 \rangle_{\beta_2}$ are found. Then, we interpolate between β_1 and β_2 .

The Plummer model ($S = 0$) requires $\langle q^2 \rangle_\beta = \frac{1}{4}$, i.e. $\beta = \frac{7}{2}$ for all stars. Mass segregated models need $\langle q^2 \rangle_\beta < \frac{1}{4}$ for massive stars and $\langle q^2 \rangle_\beta > \frac{1}{4}$ for light ones. The procedure for finding appropriate β will fail for $\langle q^2 \rangle_\beta > \langle q^2 \rangle_{-1/2} = \frac{3}{4}$ which, however, is not required even for the lightest star in the model with $S = 0.5$.

REFERENCES

- Aarseth S. J., 2003, Gravitational N-Body Simulations, Cambridge University Press
- Aarseth S. J., Hénon M., Wielen R., 1974, A&A 37, 183
- Baumgardt H., Heggie D. C., Hut P., Makino J., 2003, MNRAS 341, 247
- Bonnell I. A., Bate M. R., 2006, MNRAS 370, 488
- Capuzzo Dolcetta R., Di Matteo P., Mocchi P., 2005, AJ 129, 1906
- Chandrasekhar S., 1942, Principles of stellar dynamics, Chicago, University of Chicago Press
- Da Costa G. S., Freeman K. C., 1976, ApJ 206, 128
- Fischer P., Pryor C., Murray S., Mateo M., Richtler T., 1998, AJ 115, 592
- Gunn J. E., Griffin R. F., 1979, AJ 84, 752
- Hillenbrand L. A., Hartmann L. W., 1998, ApJ 492, 540
- King I. R., 1965, AJ 70, 376
- Kroupa P., 2007, astro-ph/0708.1164
- Kroupa P., 2001, MNRAS 322, 231
- Lynden-Bell D., Eggleton P. P., 1980, MNRAS 191, 483
- McMillan S. L. W., Vesperini E., 2007, ApJ 655, L45
- Mocchi P., 2006, MNRAS 366, 227
- Murray S. D., Lin D. N. C., 1996, ApJ 467, 728
- Spitzer L., 1969, ApJ 158L, 139
- Stolte A., Brandner W., Brandl B., Zinnecker H., 2006, AJ 132, 253